

## Large-Scale Convergence in a Numerical Cloud Model

SIMON W. CHANG AND HAROLD D. ORVILLE

*Institute of Atmospheric Sciences, South Dakota School of Mines and Technology, Rapid City 57701*

30 May 1972 and 4 April 1973

### 1. Introduction

The purpose of this note is to explain one way that the effects of larger scale horizontal convergence-divergence patterns can be superimposed on a numerical cloud model and to illustrate the results of one such superposition. As such it concentrates on the effects of the larger scale motions on the smaller scale motions.

The severity of local-scale circulations often depends upon the larger scale flow. In middle latitudes, hailstorms and squall lines have been correlated with upper air disturbances moving through an area (Longley and Thompson, 1965; Schleusener, 1962; Ferguson, 1967). A plausible explanation is that the mechanism responsible for the intensification is connected with the low-level convergence, high-level divergence patterns which lead, primarily, to moisture additions in the lower atmosphere at a rate considerably in excess of that due to evaporation from lakes or vegetated land. In lower latitudes, some scientists consider that the large clouds in the tropics or, in fact, almost any cloud development in the tropics requires some larger scale convergence to initiate the cloud growth. This is because a rather uniform surface exists under the clouds, unless in the area of islands, and inhomogeneities in the lower surface cannot be counted on to supply the initial perturbation for cloud growth as in continental regions. The following gives our treatment of a streamfunction formulation which simulates larger scale convergence-divergence in a two-dimensional cloud model and then briefly discusses the results in one case. It appears that this type of boundary layer convergence will also be necessary in three-dimensional models in which, however, streamfunctions will probably not be used.

### 2. The model

A streamfunction is utilized in a model which simulates cumulonimbus clouds in a tropical atmosphere. The initial thermodynamic conditions are shown in Fig. 1. The model is two dimensional, 20 km wide by 20 km high, with equal grid intervals of 200 m in the *x*- and *z*-directions. The governing equations have been developed by Orville and others (Ogura and Phillips, 1962; Orville, 1965) with recent developments concerning the ice phase reported at

several meetings and in a lengthy report,<sup>1</sup> and in one paper (Wisner *et al.*, 1972). Principal modifications to the earlier work are an extension to deep convection, an iterative process to determine saturation in place of Ogura's technique, and nonlinear eddy coefficients in place of constant coefficients. The clouds are produced by random perturbations in temperature and water vapor with maximum possible amplitudes of 2C and 2.5 gm kg<sup>-1</sup>, respectively, introduced every 20 min of simulated real time. The same random numbers are used each 20-min interval. The perturba-

<sup>1</sup> Orville, H. D.: Convective clouds and their interactions with the lower boundary layer. Presented at the Mesoscale Observing Network Meeting, 25-26 May 1971, Texas A&M; Orville, H. D., and S. W. Chang: Numerical simulation of hurricane rainband clouds. Presented at the 7th Technical Conference on Hurricanes and Tropical Meteorology, 6-9 December 1971, Barbados, West Indies; Chang, Simon W., and Harold D. Orville: Modification of hurricane rainband clouds and numerical simulation. Presented at the 3rd Conference on Weather Modification, June 1972, Rapid City, S. D.; Orville, H. D., S. W. Chang and F. J. Kopp, 1972: A numerical experiment on the simulation and modification of hurricane rainband clouds. Rept. 72-12, Institute of Atmospheric Sciences, South Dakota School of Mines and Technology.

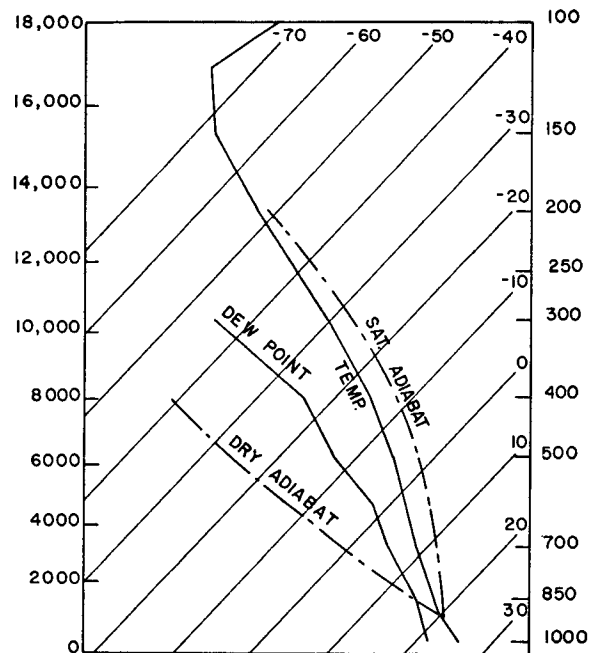


FIG. 1. Portions of the skew *T*-log *P* chart showing the initial thermodynamic conditions.

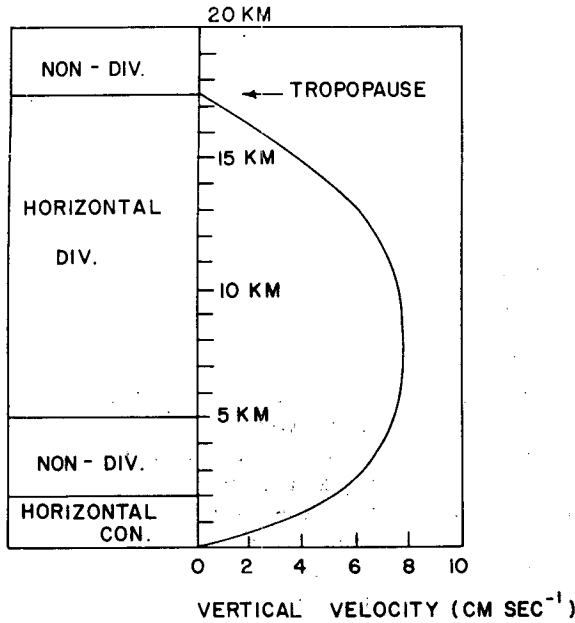


FIG. 2. Initial large-scale vertical velocity and horizontal divergence distribution in Case 1.

tions are introduced in the right half of the grid over a depth of 600 m (from 600 to 1200 m). Ambient airflows from right to left in the lower atmosphere and from left to right in the upper atmosphere are initially prescribed, in an attempt to model conditions appropriate to hurricane rainband clouds. Hence, the grid domain is perpendicular to the hurricane circulation, with the eye 150–200 km to the left of the grid. Slight upward motions are superimposed (of the order of centimeters per second) in some cases. The streamfunction values are kept constant at the side boundaries. No vertical motion is allowed at the bottom and top boundaries. Other dependent variables are allowed to vary with time so that horizontal gradients at the side boundaries are zero, as in Orville (1968).

3. Streamfunction formulation

The initial streamfunction value in a case with no horizontal convergence is generated by the expression

$$\psi_0(z) = -Az - \frac{B_i}{2}z^2.$$

The constant  $A$  represents the momentum of the horizontal flow at  $z=0$  which equals numerically the product of the horizontal wind speed and the air density at  $z=0$ . In our case, a value of  $-5 \text{ m sec}^{-1}$  times the initial horizontally stratified air density at  $z=0$  ( $1.0 \text{ kg m}^{-3}$ ) is used for  $A$ . At any level  $z$ ,  $B_i$  is the vertical gradient of the horizontal momentum, which equals numerically the product of the assumed vertical wind shear and the initial air density at  $z$ . A value of  $5.71 \times 10^{-4} \text{ sec}^{-1}$  times the initial horizon-

tally stratified air density at different heights is used for the  $B_i$ 's for  $z \leq 17.5 \text{ km}$ ;  $B_i=0$  above 17.5 km. The  $B_i$ 's represent a piecewise continuous function, constant at any height interval. The wind profile in our case is then  $-5 \text{ m sec}^{-1}$  at  $z=0$ , increasing to  $5 \text{ m sec}^{-1}$  at  $z=17.5 \text{ km}$ , and then a constant  $5 \text{ m sec}^{-1}$  above 17.5 km (tropopause) at 20 km, the top of the model. The relationships for  $u$  and  $w$  are

$$\rho_0 u = -\frac{\partial \psi}{\partial z}, \quad \rho_0 w = \frac{\partial \psi}{\partial x} \tag{1}$$

Therefore

$$\rho_0 u = A + Bz, \quad w = 0,$$

where  $\rho_0(z)$  is the initial stratified air density.

In a case with superimposed horizontal convergence, the streamfunction value is generated by

$$\psi(x, z) = \psi_0(z) + C_1 x z',$$

with

$$z' = \begin{cases} 0, & z > z_0 \\ z, & z \leq z_0 \end{cases}$$

where  $z_0$  is the depth of boundary layer, and  $C_1$  the magnitude of the superimposed horizontal convergence, i.e.,

$$\frac{\partial \rho_0 u}{\partial x} = \begin{cases} -C_1, & z \leq z_0 \\ 0, & z > z_0 \end{cases}$$

By (1), the general upward motion initiated by this horizontal convergence in the boundary layer is

$$w = C_1 z / \rho_0.$$

Hence, the horizontal convergence is compensated by the vertical divergence at every point given by

$$\nabla \cdot \rho_0 \mathbf{V} = \frac{\partial \rho_0 u}{\partial x} + \frac{\partial \rho_0 w}{\partial z} = -C_1 + C_1 = 0.$$

For mass conservation in the model, horizontal divergence must be superimposed in the upper levels of the model. The streamfunction is then generated by

$$\psi(x, z) = \psi_0(z) + C_2 x z',$$

with

$$z' = \begin{cases} z - z_1, & z_1 \leq z \leq z_2 \\ 0, & \text{otherwise} \end{cases}$$

where  $z_2 - z_1$  is the depth of horizontal divergence layer and  $C_2$  is the magnitude of the divergence given by

$$C_2 = -\frac{z_0 C_1}{z_2 - z_1}.$$

Thus, the total mass convergence in the model is zero. In our study, the magnitude of  $C_1$  is approximately  $5 \times 10^{-5} \text{ kg m}^{-3} \text{ sec}^{-1}$  with  $z_0 = 1 \text{ km}$ ,  $z_1 = 5 \text{ km}$  and

$z_2 = 17.5$  km. This gives a vertical velocity of  $5 \text{ cm sec}^{-1}$  at 1 km, increasing to  $8 \text{ cm sec}^{-1}$  at 6.5 km due to the decrease in density with height, and then decreasing to zero at 17.5 km. Fig. 2 shows this (Case 1) vertical velocity variation with height and the corresponding horizontal divergence distribution. This upward flow causes a general cooling with maximum rate of  $0.3\text{C hr}^{-1}$  in the atmosphere, which is, of course, insignificant compared with the warming or cooling produced by the phase change of water in clouds.

**4. An example**

Figs. 3 and 4 illustrate the development of clouds in two cases. The first (Fig. 3) shows a case in which horizontal convergence (of magnitude  $5 \times 10^{-5} \text{ kg m}^{-3} \text{ sec}^{-1}$ ) is sufficient to give vertical velocities of  $5 \text{ cm sec}^{-1}$  at 1 km, the top of the boundary layer. No horizontal convergence or divergence is modeled in Case 2 (Fig. 4). The initial vertical velocities are zero. All other initial and boundary conditions are identical in the two cases.

In both cases, clouds are initiated by perturbations after a few time steps, but no convective cloud associated with appreciable updrafts appears until after 50 min.

In Case 1, cloud tops ascend at  $100 \text{ m min}^{-1}$  after 50 min to attain a height of 8 km at 108 min. Fig. 3 illustrates the cloud outlines and the rain and precipitating ice distributions at 108 min. The clouds at the 7-km level beside the main cell are caused by the general upward motion initiated by the boundary

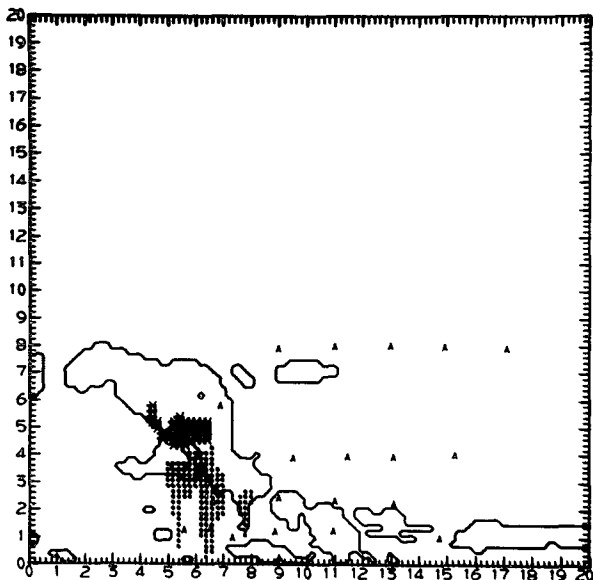


FIG. 3. Cloud outlines and precipitation at 108.25 min for Case 1, a case with horizontal convergence in the lower 1 km and divergence from 5 to 17.5 km. The dots denote rain with water content over  $1 \text{ gm kg}^{-1}$ , the asterisks precipitating ice content over  $1 \text{ gm kg}^{-1}$ , and the A's air parcels used to trace motions in the model. The numbers on the ordinate and abscissa denote kilometers.

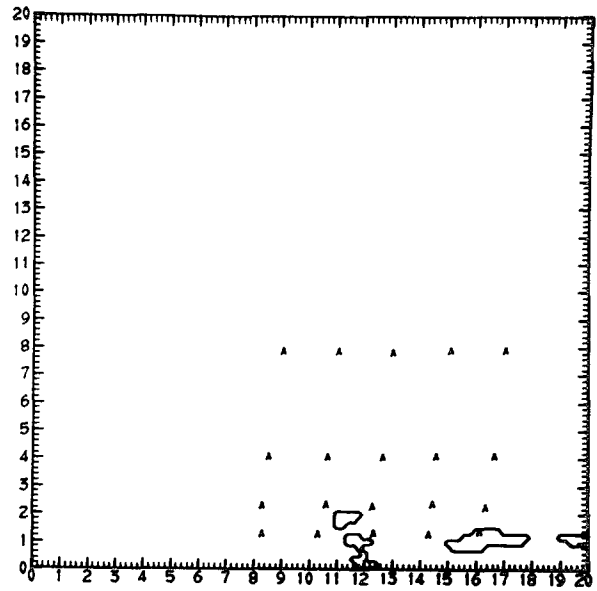


FIG. 4. Same as Fig. 1 but for Case 2 with no convergence or divergence superimposed.

layer convergence. The clouds evident below 3 km are produced by successive perturbations and are possible embryos of larger cells.

Fig. 4 demonstrates the same situation for Case 2 as Fig. 3 does for Case 1. Small, inactive cells exist. The convective cells found at the right have grown to 2.5 km which is 5.5 km lower than the main cell in Case 1 at the same time. The maximum updraft in Case 1 reaches  $8 \text{ m sec}^{-1}$ , while in Case 2 is only  $3 \text{ m sec}^{-1}$ . Active cloud growths in Case 1 have diameters of at least 2 km whereas the clouds in Case 2 are normally about 1 km in width. Hence, the simulated boundary layer convergence leads to broader, more active clouds cells.

The physical reason for this more active convection seems obvious. The superimposed upward motion in the boundary layer causes cooling and moistening of the atmosphere. The cooling rate is small, as mentioned earlier. The large-scale upward flow creates an average moistening rate of  $1.8 \times 10^{-4} \text{ gm kg}^{-1} \text{ sec}^{-1}$  which in 100 min would advect an additional  $1 \text{ gm kg}^{-1}$  of water vapor to the 1-km level. The random numbers generated are exactly the same for the two cases but will operate on slightly different fields (10% greater water content in regions of strongest upward motion in Case 1). Thus, the clouds are formed by slightly different hydrothermal perturbations but still, we think, must owe the major part of their additional growth to the modified stability of the environment.

**5. Conclusions**

Our results suggest that larger scale convergence is an important parameter to introduce into numerical cloud models particularly if forecasts of an hour or

more are to be made. The question next arises as to what values should be used. In our area of the Black Hills, numerical models such as Lavoie (1972) has developed could be used to supply values of convergence in the boundary layer for airflow over the Black Hills. Pilot balloon observations or other models may be applicable for determining the boundary layer convergence. In any event, some effort should be made by observers and modelers to specify the larger scale convergence in an area if predictions of cloud development are to be made, as opposed to purely dynamic studies of cloud growth over a few tens of minutes.

*Acknowledgments.* This work is sponsored by the National Hurricane Research Laboratory, under NOAA Grant N22-3-72(g). We thank Alex Koscielski for pointing out the need for considering larger scale convergence in our numerical cloud models and Prof. Jule Charney for criticizing our earlier tropical cloud models for the same defect.

The calculations were done at the Computing Facility of the National Center for Atmospheric

Research, which is sponsored by the National Science Foundation.

#### REFERENCES

- Ferguson, H. L., 1967: Mathematical and synoptic aspects of a small-scale wave disturbance over the lower Great Lakes area. *J. Appl. Meteor.*, **6**, 523-529.
- Lavoie, R. L., 1972: A mesoscale numerical model of lake-effect storms. *J. Atmos. Sci.*, **29**, 1025-1040.
- Longley, R. W., and C. E. Thompson, 1965: A study of the causes of hail. *J. Appl. Meteor.*, **4**, 69-82.
- Ogura, Y., and N. A. Phillips, 1962: Scale analysis of deep and shallow convection in the atmosphere. *J. Atmos. Sci.*, **19**, 173-179.
- Orville, H. D., 1965: A numerical study of the initiation of cumulus clouds over the mountainous terrain. *J. Atmos. Sci.*, **22**, 684-699.
- , 1968: Ambient wind effects on the initiation and development of cumulus clouds over mountains. *J. Atmos. Sci.*, **25**, 385-403.
- Schleusener, R. A., 1962: On the relation of the latitude and strength of the 500 mb west wind along 110°W longitude and the occurrence of hail in the lee of the Rocky Mountains. Colorado State University, Atmos. Sci. Tech. Paper No. 26.
- Wisner, C., H. D. Orville and C. G. Myers, 1972: A numerical model of a hail-bearing cloud. *J. Atmos. Sci.*, **29**, 1160-1181.